Progress in Natural Science: Materials International 2012;22(2):79–85

Chinese Materials Research Society

Progress in Natural Science: Materials International

www.elsevier.com/locate/pnsmi
www.sciencedirect.com

ORIGINAL RESEARCH

Transparent anatase titania films: A critical study on optical properties

P.K. Manoj[a,*], P. Koshy[b], V.K. Vaidyan[b]

[a] *VIT University, Vellore, Tamilnadu, India*
[b] *Department of Physics, University of Kerala, Trivandrum 695581, India*

Received 23 January 2012; accepted 22 February 2012
Available online 17 April 2012

KEYWORDS

Thin films;
Optical properties;
Electron beam deposition

Abstract Titania thin films are prepared by electron beam evaporation and deposition conditions are optimized. X-ray diffraction studies have shown a polycrystalline nature of the films with anatase phase. The preferential orientation as well as electro-optical properties are found to be sensitive to substrate temperature. The structural and optical studies carried out on this high refractive index material give ample evidence for its columnar and porous structure. The analytical expressions enabling the derivation of optical constants from its transmission spectrum only, have successfully applied. Finally, the refractive index dispersion is discussed in terms of the single-oscillator Wimple and DiDodmenico model.

1. Introduction

Thin film titania (TiO_2) is a versatile material and therefore has been the subject of sustained research interest. Its diverse applications include high dielectric capacitors in random access memory, electroluminescent devices, transparent protective coatings on silica optical fibers, antireflective coatings for Si solar cells, deep ultraviolet lithography, high refractive index component of multilayers for optical antireflectors, soft X-ray reflectors, gas sensors and electrochromic devices [1]. The electrical and optical properties depend upon refractive index, wide band gap and chemical stability while dielectric constant depends upon atomic structure. However, titania thin film with rutile structure is known as good blood compatible material and can be used in artificial heart valves [2]. Many different technique can be used for film fabrication viz., evaporation [3,4], sol–gel [5], metal organic chemical vapor deposition [6], sputtering [7], atomic layer deposition [8] and laser abalation [9].

Bulk crystalline titania at atmospheric pressure and room temperature has three polymorphous: rutile, anatase and brookite. Rutile is thermodynamically most stable phase,

*Corresponding author. Tel.: +91 9843558727.
E-mail address: pkmanoj@gmail.com (P.K. Manoj).

Peer review under responsibility of Chinese Materials Research Society.
http://dx.doi.org/10.1016/j.pnsc.2012.03.011

Production and hosting by Elsevier

while anatase and brookite exist as metastable phases below 1100 K. Titanium is in octahedral coordination with oxygen as TiO_6 units in all polymorphs. However different Ti-O bond lengths and angles and consequently different arrangements of TiO_6 octahedra, generate different lattice structures. The rutile and anatase lattices are tetragonal with $P4_2/mnm$ and $I4_1/amd$ space groups, while brookite is orthorhombic with Pbca symmetry [10].

Titania thin films exist in four forms: rutile, anatase, brookite and amorphous [11,12]. In samples prepared by electron beam evaporation only anatase, rutile and amorphous phases are found. The microstructure and properties of films depend upon details of deposition parameters which determine nucleation and growth of crystal phase. When TiO_2 is taken as evaporation material the anatase phase is sometime found for substrate temperatures above 523 K, while evaporation of Ti and TiO produce anatase and rutile mixture above 583 K [13]. Films deposited below these respective temperatures are generally amorphous. The main parameters for evaporation process are substrate temperature, deposition rate and oxygen partial pressure. The transparency of titania thin films is highly sensitive to loss of oxygen which causes absorption in near infrared region extending into the visible and yields a blue coloration. The properties of titania films depend not only on the preparation technique but also on the deposition condition. An attempt has been done in this study to relate the effect of substrate temperature on the composition, structural, electrical and optical properties of the films. Such detailed understanding of the film properties is necessary, if titania films are to be developed to a degree which will enable its use in various devices.

2. Experimental

The films were deposited by electron beam evaporation of TiO_2 powder (99.5%) in a 12 in. high vacuum chamber pumped with a diffusion pump. The base pressure before deposition was 10^{-6} mbar and oxygen was admitted through a needle valve into the chamber until the vacuum is reduced value. The optimum deposition conditions, which are summarized in Table 1 are attained by the design of the experiment methodology described by Wiley [14]. The thickness of the film and the rate of deposition are monitored and controlled by digital thickness monitor equipped with quartz crystal oscillator. The substrate temperature (T_s) is varied from ambient to 773 K with an accuracy of ± 5 K. The substrates were heated by resistive heating method and T_s was measured with chromal–alumel thermcouple, which was attached to lower side of one of the substrates. The thin films having 110 nm thickness were deposited on glass substrates at a deposition rate of 0.5 Å/s, located at 15 cm from the source.

Table 1 Optimum deposition conditions.

Deposition parameters	Optimum condition
Starting material	TiO_2 (99.9%)
Soaking time	3 min
Soaking power	<250 W
Deposition rate	0.5 Å/s
Deposition pressure	5×10^{-5} mbar
Source to substrate distance	15 cm
Film thickness	110 nm
Substrate temperature	723 K

Crystallinity and phase analysis of the films were carried out by a Philips PW 1830 X-ray diffraction spectrometer with an accelerating potential 40 kV and current 30 mA using $CuK_{\alpha1}$ radiation (1.54056 Å) as an X-ray source which is equipped with Ni filter. All peaks were recorded at a scanning rate of $1^\circ\,min^{-1}$ in steps of 0.03° in the standard θ–2θ geometry. The data was acquired over the $2\theta=20^\circ$–70° range because reference diffraction patterns for the titania polymorphous show that all the first order peaks occur in this interval. Surface morphological studies were carried out by JEOL JSM 5600 LV scanning electron microscope with an accelerating potential of 20 kV. The elemental composition of the samples was studied using EDAX make energy dispersive spectrometer attached to the SEM. The resistivity studies were done using a four probe set-up and transmission studies using Ocean Optics make single channel spectrometer PC 1000 in the range 300–800 nm.

3. Results and discussion

3.1. Growth mechanism

The electrical, optical and structural properties of the thin films have strong dependence on the stoichiometry and microstructure as well as the level of residual stress caused by deposition techniques and interaction with substrate [15]. In electron beam evaporation thin film deposition can be considered to be a process of impingement of deposit species on a substrate, the nucleation of clusters and the agglomeration of these clusters into a continuous film. The atoms or molecules arriving from vapor into the substrate will not all stick to the surface; there will always be a fraction of incident flux that will immediately re-evaporate. For those atoms that condense on the surface, the next stage of film growth involves migration over the substrate prior to atoms bonding together to form a deposit nucleus. If the substrate temperature and kinetic energy of incident atoms are both low, then amount of surface migration, may be very limited, atoms remain roughly in the position of the substrate where they arrived from vapor phase. Under these circumstances an amorphous deposit layer will normally be formed as the individual atoms will not have sufficient energy even to arrange themselves into the equilibrium crystalline structure. High growth rate and low substrate temperature favours the formation of amorphous films. This is because the time available for the layer of deposit of atoms to relax into crystalline lattice before being covered by subsequent layer is small and mobility of atoms over the surface is also low. The mobility of deposit atoms depends partly on the incident kinetic energy of deposit species as high incident kinetic energy may induce surface migration even when the surface migration is cold. The strength of the interaction of deposit atoms with substrate may also influence the temperature of the amorphous/crystalline transition. Hence, in order to deposit anatase titania films, deposition rate is reduced to 0.5 Å/s and substrate temperature is kept above 573 K.

At an oxygen partial pressure of 1×10^{-4} mbar, the prepared films are black, indicating the high concentration of

oxygen vacancies. The specimen prepared between an oxygen partial pressure of 7×10^{-5} and 1×10^{-5} mbar are clear. Even though the property variation of the films due to partial pressure variation is not the subject of this article, Mergel et al. [13] reported that, the color change of films prepared at different partial pressures is correlated with the density of films. This is further correlated with the decrease of mean free path in deposition chamber and a corresponding thermalization of the following reasoning. In the classical kinetic theory of gases the mean free path λ is given by [16]

$$\lambda = \frac{RT}{N_A \sigma p \sqrt{2}} \tag{1}$$

where $N_A = 6.022 \times 10^{23}$ mol^{-1} is the Avogadro's constant and σ is the collision cross section of the participating atoms and molecules. Here, the collision particles are Ti, TiO and O_2 having $\sigma \cong 0.46$ nm^2. For $T = 300$ K Eq. (1) transforms to

$$\lambda p = 6.3 \times 10^{-3} \text{ mbar cm} \tag{2}$$

For collision of evaporated species the background gas temperature is not defined. We try to estimate it for the films prepared at 5×10^{-5} mbar. Let us assume that the mean free path is 525 cm. This yields $\lambda p = 26.25 \times 10^{-3}$ mbar cm corresponding to collision temperature of 300 K $\times$ 26.25/6.3 = 1250 K. This seems to be reasonable, between the temperatures of background gas >300 K and that of the evaporated species >2500 K, somewhat higher than the melting temperature. Hence, it is reasonable to assume that at 5×10^{-5} mbar, the evaporated species have good thermalization.

3.2. Microstructural analysis

The X-ray diffraction of titania films deposited at different substrate temperatures are compared with JCPDS files no. 21-1271, and the results are presented in Table 2. The films deposited at room temperature show amorphous nature, while the films deposited above 573 K show a crystalline nature. As the substrate temperature increases above 573 K, the preferential orientation along (101) crystal plane with $2\theta = 25.18^{\circ}$ becomes evident. However, all peaks have low intensity suggesting that the amorphous titania co-exists along the crystalline phase [11].

Table 2 Structural parameters of titania films prepared at different substrate temperatures.

Substrate temperature (K)	Angle ($2\theta^{\circ}$)	Lattice spacing d (Å)	Identification		Lattice parameter	
			Phase	(hkl)	a (Å)	c (Å)
573	53.5	1.71	TiO_2	105	–	–
623	25.18	3.53	TiO_2	101	3.81	9.51
	37.81	2.38	TiO_2	004		
	53.84	1.70	TiO_2	105		
673	25.29	3.52	TiO_2	101	3.79	9.48
	37.91	2.37	TiO_2	004		
	54.01	1.66	TiO_2	105		
723	25.69	3.51	TiO_2	101	3.77	9.48
	37.94	2.37	TiO_2	004		
	54.08	1.69	TiO_2	105		
773	25.38	3.51	TiO_2	101	3.77	9.51
	37.18	2.38	TiO_2	004		
	54.12	1.69	TiO_2	105		
JCPDS					3.78	9.514

The surface morphology micrographs of titania films are shown in Fig. 1. The micrograph of as-deposited film prepared at room temperature shows, its amorphous nature morphologically, which is in support of the XRD analysis. The surface morphology of titania films prepared at $T_s = 573$ K, reveals the formation of crystallites. It can be seen that when the substrate temperature of the films reaches 673 K, there is a distinct change in surface morphology. The micrograph of films prepared at 673 K shows column like nodules having a size of particles in the range 150–300 nm. The formation of non-uniform grains over the substrate with voids between them indicates porosity. SEM photograph shows more evenly arranged column like nodules having almost uniform size (300 nm), which is formed at 723 K. More keen edged grains are observed in films formed above 723 K. Hou et al. [17], reported formation of similar grains in titania films with increase of substrate temperature.

EDS analyses of the samples were done at different places of samples and it was found that the composition of samples is uniform throughout the samples. From the change of peak area, the variation of content of oxygen and titanium and hence the non-stoichiometry is verified and O/Ti ratio is found to be varying from 2 to 1.75.

3.3. Optical properties

Fig. 2 shows the normalized optical characteristics of titania films prepared at different substrate temperatures in the wavelength region 300–800 nm. It is clearly observed that the films are transparent in region above 400 nm. However, all films have weak absorption and interference fringes in the region 400–800 nm range and have large amplitude. It is well known that the amplitude of interference fringes is a measure of film quality, meaning larger the amplitude, better is the film. The interference fringes are the result of interference of light reflected between the air–film and film–substrate interfaces. In the present set of samples, interference effect also becomes prominent. This may be due to re-arrangement of crystallites/grains as discussed earlier, or because of porous structure of the films.

The absorption coefficient (α), in spectral region of high absorption is calculated using the relation

$$\alpha = \frac{1}{t} \ln(1/T) \tag{3}$$

where T is transmittance and t is film thickness.

The fundamental absorption edge of most semiconductors is characterized by an exponential variation of the absorption coefficient with photon energy. The absorption has its minimum at low energy and increases with optical energy. The variation of absorption coefficient with photon energy of the deposited films is depicted in Fig. 3. Near absorption edge, absorption coefficient increases more rapidly with $h\nu$. From Fig. 3 it is clear that the variations in substrate temperature affect both the magnitude and shape of α–$h\nu$ curve, but absorption edge of anatase is found to be of the Urbach type.

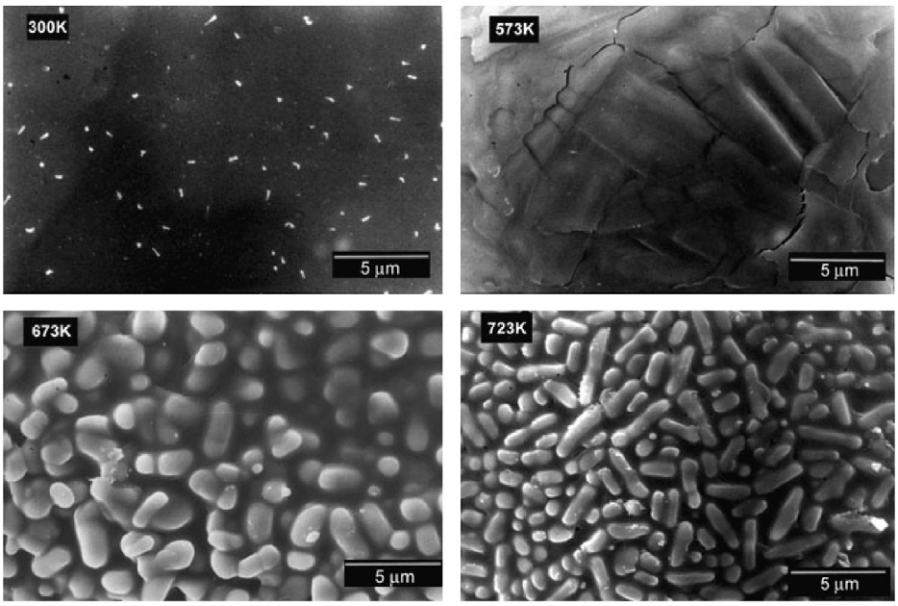

Fig. 1 SEM micrographs of titania thin films deposited at different substrate temperatures.

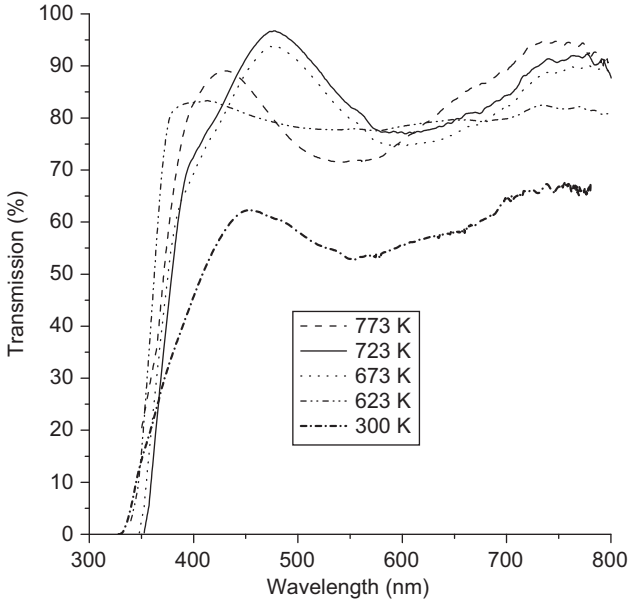

Fig. 2 Optical characteristics of titania thin films.

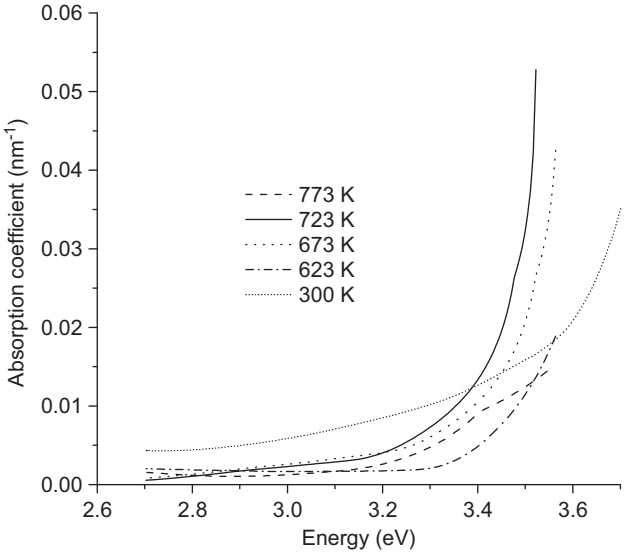

Fig. 3 Variation of absorption coefficient with energy.

The absorption coefficient (α) of a crystalline solid obeys the following relationship

$$\alpha h\nu \propto (h\nu - E_g)^p \tag{4}$$

where E_g is the optical band gap, $h\nu$ is the photon energy and p being the index which characterizes the optical absorption process. For direct allowed transitions, $p=1/2$ for direct forbidden transition $p=3/2$ for indirect allowed transition $p=2$ and finally for indirect forbidden transition $p=3$.

An analysis of absorption data was carried out to determine the predominant optical transition. According to the power law Eq. (4), Fig. 4 represents a plot between $(\alpha h\nu)^{1/2}$ and $h\nu$. The points lie close to one straight line for $E_g - x < h\nu < E_g + x$ to a steeper line for $h\nu > E_g + x$ where x represents the energy due to phonon transition. This behavior is just what one can expect if the absorption in this range is due to indirect transition in which there is a marked change in momentum between the initial and final states in which direct transition do not play a role. Accordingly, the value of $p=2$ and hence the type of transition is allowed indirect [18]. The allowed indirect process, which involves practically no transition between localized steps, is the responsible mechanism for optical excitation in titania films [19].

The variation of optical energy gap with variation of substrate temperature is presented in Table 3. From the data presented, it is evident that, the optical energy gap decreases with increase in substrate temperature. In other words, this result is in agreement with the phase transition and/increment of anatase phase volume in titania films with substrate temperature. Similar results are reported earlier [11].

From the measured optical transmittance, refractive index, optical absorption and extinction coefficient of the films are

calculated using the envelope method [20]. The envelope is drawn in the figure and is evident that for every wavelength λ, there is a corresponding maximum transmittance T_M and a minimum transmittance T_m. The transmittance T at any wavelength is a function of refractive index n, its extinction coefficient k and thickness t of the film, has the general form

$$T = \frac{Ax}{B - Cx\cos\phi + Dx^2} \tag{5}$$

where $A = 16s(n^2 + k^2)$,

$B = \left[(n+1)^2 + k^2\right]\left[(n+1)(n+s^2) + k^2\right]$,

$C = 2\left[(n^2 - 1 + k^2)(n^2 - s^2 + k^2) - 2k^2(s^2+1)\right]\cos\phi$
$\quad -2\left[2(n^2 - s^2 + k^2) + (s^2+1)(n^2 - 1 + k^2)\right]\sin\phi$,

$D = \left[(n-1)(n-s^2) + k^2\right]\left[(n-1)^2 + k^2\right]$,

$x = \exp(-\alpha t)$,

$\alpha = \frac{4\pi k}{\lambda}, \quad \phi = \frac{4\pi nt}{\lambda}$

and s = refractive index of the substrate. (6)

Eq. (5) is valid only if the film is homogenous, thickness of the film is uniform and the substrate is semi infinite and completely transparent i.e. $k_s(\lambda) = 0$. The equations describing the envelope method can be derived from Eq. (5), with further assumptions: (i) the square of the refractive index of the film is much higher than that of the extinction coefficient of the film, i.e., $n^2 \gg k^2$, and (ii) the square of the refractive index difference between film–air and film–substrate is much greater than that of the extinction coefficient of the film in $(n-1)^2 \gg k^2$ and $(n-s)^2 \gg k^2$.

The first assumption leads to $A = 16n^2$s and $B = (n+1)^3(n+s^2)$ in Eq. (5). The second assumption leads to $C = 2[(n^2-1)(n^2-s^2)]\cos\phi$ and $D = (n-1)^3(n-s)^2$. The most critical assumption of these is $(n-1)^2 \gg k^2$. In the present study for titania films, the refractive index is greater than 2 and that of the substrate is 1.5. Therefore if $k^2/(n-s)^2 \leq 0{\cdot}01$, and if $n = 2$ and $s = 1.5$, k must be less than 0.05.

With above assumptions, the constants in Eq. (5) assume the above mentioned values. The cosine function in the denominator oscillates between +1 and −1, which results in

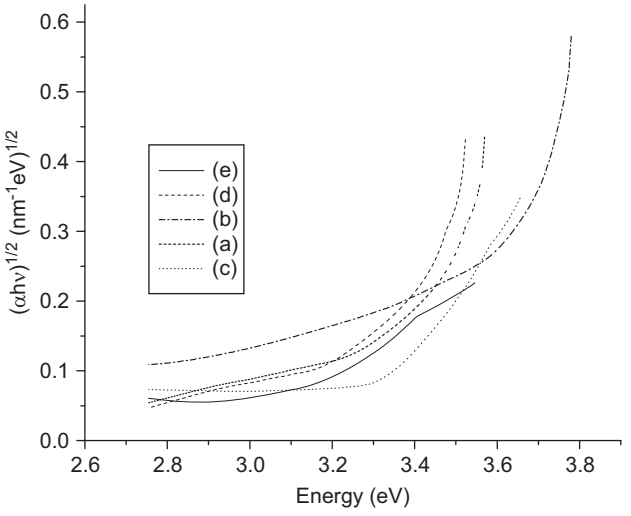

Fig. 4 Variation of $(\alpha h\nu)^{1/2}$ with photon energy for films prepared at (a) 300, (b) 573, (c) 673 (d) 723 and (e) 773 K.

well known equation for the interference fringes in transmission spectrum.

$$2nt = m\lambda \tag{7}$$

where the order number m is an integer for maxima and a half integer for minima.

Hence, the extreme interference fringes T_M and T_m can be written as

$$T_M = \frac{Ax}{B - Cx + Dx^2} \tag{8}$$

and

$$T_m = \frac{Ax}{B + Cx + Dx^2} \tag{9}$$

respectively.

From Eqs. (8) and (9), the refractive index

$$n = [N + (N^2 - s^2)^{1/2}]^{1/2} \tag{10}$$

where $N = \frac{1+s^2}{2} + \frac{2s}{T_M T_m}(T_M - T_m)$

and $x = E_M - \frac{[E_M^2 - (n^2-1)^3(n^2-s^4)]^{1/2}}{(n-1)^3(n-s^2)}$

where $E_M = \frac{8n^2 s}{T_M} + (n^2-1)(n^2-s^2)$. (11)

Once T_M and T_m are obtained from measured transmission spectrum and refractive index of substrate is known, the refractive index of the film can be calculated from Eq. (10).

The equations derived above, from the envelope method assumes that the substrate is semi-infinite. Since, if the specimen consists of a film, on a thick substrate, the light intensity loss from the back surface must be taken into account [21].

Considering the back surface of the substrate into account, the transmittance T', of the film as the finite substrate can be approximated as

$$T' = T(1-r) \tag{12}$$

where r is the reflection at the air–back substrate surface which is equal to $(s-1)^2/(s+1)^2$. For Eq. (10), T is the transmittance of the film on a semi-infinite substrate. Starting from Eq. (10) and following the procedure to solve Eq. (5), the solutions found to have exact form as Eqs. (10) and (11). The only difference appears in N due to the extra factor of $(1-r)$ which becomes

$$N = \frac{1+s^2}{2} + \frac{8s^2}{(1+s)^2}\frac{T_M - T_m}{T_M T_m} \tag{13}$$

while comparing the method developed, by Swanepoel [20] and modified by Peng and Desu [21], the change in refractive index is negligible, <2%, but it will produce considerable effect on the values of extinction coefficient. This arises because, in envelope method, the reflection loss from back surface of substrate is counted into the extinction coefficient of the film.

In the normalized spectral characteristics—Fig. 2, the gap between 100% and transmission of T_M is indicative of the light loss due to the scattering and/absorption. Based on the strength of absorption, the transmission spectrum can be divided into three regions: weak, medium and strong absorption regions. Normally, the regions at transmittance values

higher than 0.7 will be considered as weak absorption region, while the values between 0.4 and 0.7, will be considered as medium absorption region. In the present case, the region at wavelength longer than 400 nm is assigned as weak absorption region, and wavelength shorter than 400 nm is the strong absorption region.

Once T_M and T_m are obtained, the refractive index of the film can be easily calculated using Eqs. (13) and (10). The modified envelope method, as discussed above is used to calculate the refractive index values. Fig. 5 shows the refractive index characteristics of titania films as a function of wavelength. As can be seen in figure, the titania film prepared at 773 K substrate temperature, has a refractive index value of 2.154 at wavelength around 755 nm and gradually increases to a value at 2.222 at a wavelength around 431 nm. This behavior of refractive index variation, $(dn/d\lambda)<0$, is consistent with what one would expect from Kramer's–Kroning analysis. The change of value of refractive index with substrate temperature is also presented in Fig. 5. Compared to refractive index value of bulk material, the thin films show lower indices possibly due to porosity and/or stress in the film. However, the refractive indices of the films have a tendency to increase with substrate temperature, which can be correlated with transition from amorphous state to anatase/rutile phases.

The pattern of dispersion relation for refractive index is in general agreement with obtained for the titania films [22]. Values of $(n^2-1)^{-1}$ are plotted against the inverse of the

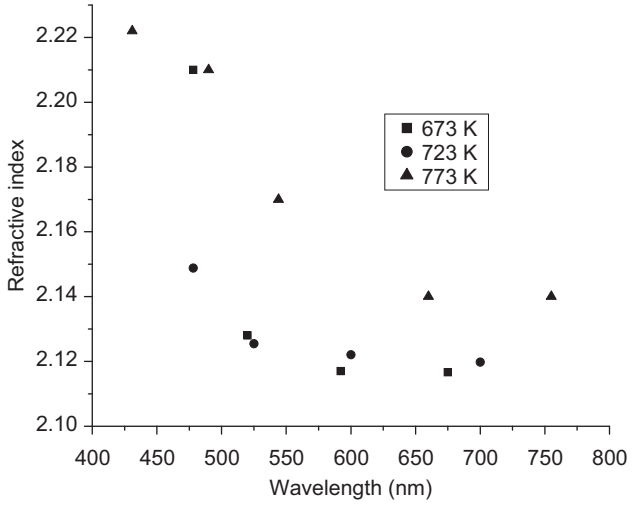

Fig. 5 Variation of refractive index of titania films prepared at different substrate temperatures with wavelength.

square of incident photon wavelength (λ^{-2}) and the dependence is found to be linear to first approximation. This explains that the dispersion relation can be explained in terms of the single oscillator model [23] as

$$n^2-1=\frac{E_dE_0}{E_0^2-(h\nu)^2} \tag{14}$$

where ν is the frequency of the incident photon energy, $h=4.13\times10^{-15}$ eV. The slope of the graph gives a value of 10^{-14} m^{-2} for average oscillator strength. Value of the single effective oscillator energy E_o and the dispersion energy E_d for interband optical transitions are estimated to be 7.38 and 24.47 eV from the zero energy intercept and slope. The coordination number N_c of the nearest titanium cation neighbor of the oxygen anion can now be found from an empirical relation between the dispersion energy E_d and the effective number of N_e of valance electron per anion as

$$E_d=2\chi N_eN_c \tag{15}$$

the factor 2 is included for the formal chemical valance of oxygen anion. $\chi=0.26\pm0.04$ for most oxides according to the oscillator model and $N_e=8$ is estimated for TiO_2 [24]. Substituting these values in Eq. (15) a value of 5.88 ± 0.9 is obtained for N_c and is appropriate for the titania films. The long wavelength limit (i.e., $\lambda^{-1}=0$) of refractive index n_∞ is found to be 2.07 using the expression

$$n_\infty=\sqrt{1+(E_d/E_0)} \tag{16}$$

This value corresponds well with the value 2.05 for titania films from magnetron sputtering [25].

Fig. 6 shows the variation of extinction coefficient with wavelength of titania films in the visible region. As discussed earlier, the extinction coefficient values are in the range as predicted from modified envelope formulation; however the order of 10^{-2} indicates good surface homogeneity [25]. The apparent oscillations in extinction coefficient seem to be correlated with the interference fringes and probably arise from small errors in the measured film thickness [26]. From this plot, one can understand the transmittance and surface roughness of the films studied. Hence, one can conclude that the optical loss due to absorption or scattering of light is very low for the prepared samples.

The variation of electrical resistivity, transmittance and figure of merit of the deposited films with substrate temperature is presented in Table 3. The films prepared at room temperature shows lowest resistivity and transparency. But, in the case of crystalline films, films deposited at 723 K shows the optimum value for figure of merit, $\phi_{TC}=T^{10}/R_{sh}$, where T is the transmittance and R_{sh} is the sheet resistance [15].

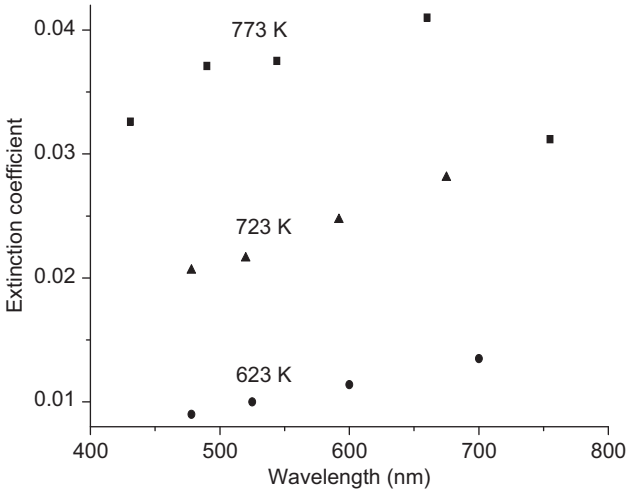

Fig. 6 Variation of extinction coefficient of titania films prepared at different substrate temperatures with wavelength.

Table 3 Electrical and optical properties of titania thin films.

Substrate temperature (K)	Resistivity (Ω m)	Band gap (eV)	Transmittance at 550 nm (%)	Refractive index at 550 nm	Figure of merit (ϕ_{TC}) ($\times 10^{-8}$ S)
Ambient	3.96×10^{-2}	3.5	53	[a]	0.486
623	2.46	3.31	78	[a]	0.373
673	0.99	3.3	80	2.12	1.19
723	3.96×10^{-1}	3.28	83	2.13	4.3
773	1.485	3.1	71	2.17	0.241

[a]Refractive index is not calculated since the envelope method is not valid for these cases.

4. Conclusions

Preparation conditions are optimized to obtain crystalline undoped titania thin films. The preferential orientations of the films formed are found to be sensitive to substrate temperature. An oxygen partial pressure of 5×10^{-5} mbar; 723 K, substrate temperature and rate of evaporation of 0.5 Å/s are found to be optimum for the deposition of good quality undoped titania films. For the films deposited under optimum deposition conditions have figure of merit 4.3×10^{-8} S and refractive index of 2.13 at 550 nm and has an indirect band gap of 3.28 eV. Beyond the band gap range, the values of refractive index decrease monotonically with increasing wavelength and approach $n_{\infty} = 2.07$.

References

[1] U. Diebold, Surface Science Reports 48 (2003) 53.
[2] F. Zhang, N. Huang, P. Yang, Surface and Coatings Technology 84 (1996) 476.
[3] H.K. Pulker, G. Paesold, E. Ritter, Applied Optics 15 (1976) 2986.
[4] W.L. Lehmann, K. Frick, Applied Optics 27 (1988) 4920.
[5] C.T. Wang, C.F. Yen, Surface and Coatings Technology 06 (2012) 262.
[6] P.K. Shin, Applied Surface Science 214 (2003) 214.
[7] B. Karunagaran, P. UthiraKumar, S.J. Chung, S. Velumani, E.K. Suh, Materials Characterization 58 (2007) 680.
[8] J. Aarik, A. Aidla, A.A. Kusler, T. Vustare, V. Sammelselg, Thin Solid Films 305 (1997) 270.
[9] X. Lie, J. Yin, Z.G. Liu, X.B. Yin, G.X. Chen, M. Wang, Applied Surface Science 174 (2001) 35.
[10] M.S. Park, S.K. Kwon, B.I. Min, Physical Review B 65 (2002) 161201.
[11] J.D. DeLoach, G. Scarel, C.R. Aita, Journal of Applied Physics 85 (1999) 2377.
[12] M.P. Moret, R.Z. Allon, D.P. Vijay, S.B. Desu, Thin Solid Films 366 (2000) 8.
[13] D. Mergel, D. Buschendorf, S. Eggert, R. Grammes, B. Samset, Thin Solid Films 371 (2000) 218.
[14] R.R. Willey, in: Practical Design and Production of Optical Thin Films, Marcel Dekker Inc., 1996.
[15] P.K. Manoj, K.G. Gopchandran, B. Joseph, P. Koshy, V.K. Vaidyan, Indian Journal of Physics 75A (2001) 507.
[16] P.W. Atkins, The Elements of Physical Chemistry, Oxford University Press, Oxford, 1992.
[17] Y.-Q. Hou, D.-M. Zhuang, G. Zhang, M. Zhao, M.-S. Wu, Applied Surface Science 218 (2003) 97.
[18] M.A. Gaffer, A.A. Fadl, Physica B 292 (2000) 221.
[19] N. Daude, C. Gout, C. Jounain, Physical Review B 15 (1977) 3229.
[20] R. Swanepoel, Journal of Physics E: Scientific Instruments 16 (1983) 1214.
[21] C.H. Peng, S.B. Desu, Journal of the American Ceramic Society 77 (1994) 929.
[22] D. Bhattachararaya, N.K. Sahoo, S. Thakur, N.C. Das, Thin Solid Films 360 (2000) 96.
[23] S.H. Wemble, H. Didomenico, Physical Review B 3 (1971) 1338.
[24] D. Mardare, P. Hones, Materials Science and Engineering B 68 (1999) 42.
[25] W. Yue, W. Zhou, Progress in Natural Science 18 (2008) 1329.
[26] J. Rodriguez, M. Gomez, J. Ederth, G.A. Niklasson, C.G. Granqvist, Thin Solid Films 365 (2000) 199.